

Tissue characterisation of atherosclerotic plaque in the left main: an *in vivo* intravascular ultrasound radiofrequency data analysis

Nestor Mercado¹, MD, PhD, FESC; Tabitha G. Moe¹, MD; Michael Pieper², MD; John A. House¹, MS; William J. Dolla¹, PhD; Lindsey Seifert¹, BS; Joshua M. Stolker³, MD; Jason B. Lindsey¹, MD; Kevin F. Kennedy¹, MS; Steven P. Marso^{1*}, MD

Saint Luke's Mid America Heart and Vascular Institute, Kansas City, MO, USA; 2. Herzzentrum Bodensee, Kreuzlingen, Switzerland; 3. Saint Louis University, Saint Louis, MO, USA

KEYWORDS

- virtual histology
- IVUS
- plaque rupture

Abstract

Aims: To characterise plaque phenotypes in the left main stem (LMS) and the proximal left anterior descending (LAD) coronary artery using virtual histology assisted intravascular ultrasound (VH-IVUS).

Methods and results: Patients with IVUS pullbacks including no less than the proximal 30 mm of the LAD and through the ostium of the left main were identified from a global IVUS registry. Plaque composition and phenotype frequency in the LMS and five consecutive non-overlapping 6 mm segments in the LAD were studied, resulting in six analysed segments per patient. There were 74 patients (72% male, mean age 65 years). The median LMS length was 5.4 mm (IQR 2.8–8.7 mm). The percent of fibrofatty plaque was greater in the LMS compared to the proximal LAD segments (27.9% [20.0-39.2] vs. 17.3% [12.2-23.1], $p < 0.001$). Dense calcium and necrotic core content was less prevalent in the LMS compared to the LAD segments (2.5% [0.9-4.7] vs. 7.9% [4.1-12.3], $p < 0.001$; and 8.0% [3.7-11.8] vs. 14% [9.2-17.9], $p < 0.001$). The frequency of thin cap fibroatheroma (TCFA) was higher in the LAD compared with LMS (0% vs. 16.9% [4.9-34.5], $p < 0.001$). Within the LAD, TCFA was most frequently observed in the second 6 mm segment, 12 mm from the ostium.

Conclusions: TCFA was present more frequently in the proximal LAD than LMS, supporting the notion that plaque rupture occurs in non-uniform locations throughout the coronary tree and preferentially spares the LMS.

*Corresponding author: Saint Luke's Mid America Heart and Vascular Institute, University of Missouri-Kansas City, 4401 Wornall Road, Kansas City, MO 64111, USA. E-mail: smarso@saint-lukes.org

Introduction

An acute coronary syndrome (ACS) usually occurs as a result of atherosclerotic plaque rupture of a coronary artery that previously was not severely narrowed¹, creating a potent stimulus for platelet aggregation, thrombus formation and arterial occlusion². Angiographic³ and intravascular ultrasound analyses (IVUS)⁴ have shown that the site of plaque rupture leading to an ACS tends to occur in predictable areas within the proximal third of the arteries and preferentially spares the left main stem (LMS) and more distal coronary segments.

Additional information from virtual histology –assisted IVUS (VH-IVUS) studies have extended these findings. Plaque composition appears to be non-uniformly distributed –principally high necrotic core content is localised to the proximal portion of the coronaries⁵. These findings can be further extended by performing plaque phenotyping. Therefore, the objective of this study was to describe the frequency of plaque phenotypes as defined by VH-IVUS in the LMS and proximal left anterior descending (LAD) in a prospective multinational VH-IVUS registry.

Methods

PATIENT SELECTION

The VH-IVUS global registry enrolled patients >18 years old and without any contraindication to IVUS imaging who underwent diagnostic or interventional coronary procedures between 2004 and 2006 at 42 multinational centres. The ethics committee of each participating institution approved the protocol, and written informed consent was obtained from all patients. Dyslipidaemia was defined as total cholesterol level ≥ 200 mg/dl, low-density lipoprotein cholesterol ≥ 100 mg/dl, high-density lipoprotein cholesterol ≤ 50 mg/dl, triglycerides ≥ 150 mg/dl, or medication use. Hypertension was defined as systolic blood pressure ≥ 140 mm Hg, diastolic blood pressure ≥ 90 mm Hg, or use of any antihypertensive drug. Diabetes mellitus was confirmed by diagnosis or use of anti-diabetic medications at study entry.

Patients underwent coronary angiography followed by IVUS at the discretion of the operator for one or more indications: 1) assessment of an indeterminate lesion, 2) investigation of a culprit lesion for optimal device sizing, 3) post-stent assessment, or 4) clarification of extent of disease.

In the present analysis, patients with analysable pre-intervention IVUS studies of the LMS (excluding the LMS bifurcation) and proximal 30 mm of the LAD, divided into equal 6 mm segments, were randomly selected (**Figure 1**). A length of 6 mm was chosen for the coronary segments located distal to the LMS carina based on the median length of LMS in the study cohort. Patients with incomplete pullback through the ostium of the LMS or <30 mm of the proximal LAD were excluded.

VH-IVUS IMAGE ACQUISITION AND ANALYSIS

Coronary vessels were imaged with 20 MHz IVUS catheters (Eagle Eye® Gold; Volcano Corp., Rancho Cordova, CA, USA) during continuous motorised pullback at 0.5 mm/s (R-100TM and Trak-Back® II; Volcano Corp.) with qualitative IVUS analysis performed

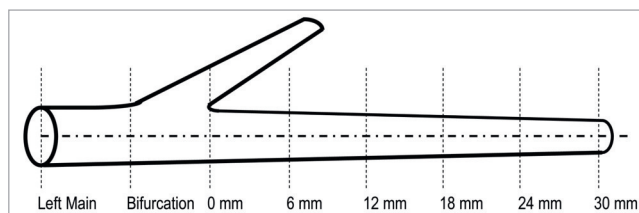


Figure 1. Intravascular ultrasound (IVUS) analysis. The proximal left anterior descending (LAD) coronary artery was divided into five 6 mm segments, the bifurcation was excluded and the left main stem (LMS) was analysed from the bifurcation to the ostium.

according to the American College of Cardiology (ACC) expert consensus on IVUS⁶. Plaque volume was derived using the Trapezoidal rule^{7,8} as follows: (external elastic membrane [EEM] volume - lumen volume). Plaque burden was defined as $([EEM \text{ area} - \text{lumen area}] / EEM \text{ area}) \times 100$. Geometric and compositional data for each frame was calculated using VH-IVUS software (pcVH V2.2; Volcano Corp.), a validated method^{9,10} that utilises the mathematical technique of autoregressive modelling to classify IVUS-radiofrequency data into one of four colour-coded plaque components: 1) fibrous (green), 2) fibrofatty (light-green), 3) dense calcium (white), and 4) necrotic core (red)¹¹⁻¹³. VH-IVUS borders were drawn by technicians at the Cleveland Clinic Department of Biomedical Engineering (Cleveland, OH, USA) or the Cardiovascular Research Foundation (New York, NY, USA) and verified at Cardialysis (Rotterdam, The Netherlands).

VH-IVUS PHENOTYPE PLAQUE CLASSIFICATION

VH-IVUS frames were assigned a plaque type by an automated pixel detection algorithm based on a modified histopathological classification scheme¹⁴ and expert consensus guidelines¹⁵ for analysing and interpreting VH-IVUS images (**Figure 2**). Interobserver variability in lesion type classification is removed by the algorithm. A confluent area of composition was defined as a circular area of the same tissue type for a minimum diameter of approximately 12 pixels or 0.08 mm² on a 400×400 VH-IVUS image. Non-atherosclerotic intimal deposits of plaque <600 μm on any VH-IVUS frame were classified as intimal medial thickening. Plaque >600 μm thick was assigned to one of four atherosclerotic phenotypes as follows: (1) pathological intimal thickening, predominantly fibrous tissue with or without >15% fibrofatty tissue and without either confluent necrotic core or confluent dense calcium; (2) fibrocalcific plaque confluent dense calcium without confluent necrotic core; (3) fibroatheroma, confluent necrotic core either not at the lumen or not exceeding 14 pixels along the circumference of the lumen on 3 consecutive frames; (4) thin cap fibroatheroma (TCFA), plaque burden (PB) >50% and confluent necrotic core extending >14 pixels along the circumference of the lumen on three consecutive frames.

STATISTICAL ANALYSIS

The statistical analysis was performed using the SAS 9.2 software package (SAS Institute, Cary, NC, USA). Continuous and cate-


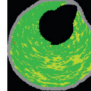
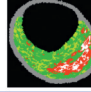


Lesion type	Brief description	Sample frame
AIT	<600 µm thick, nonatherosclerotic ("intimal xanthoma")	
PIT	>600 µm thick, predominantly fibrous tissue with or without >15% lipid pools; no calcium/necrosis	
FA	>600 µm thick, confluent necrotic core ≤14 pixels along lumen	
TCFA	>600 µm thick, >50% plaque burden and confluent necrotic core extending >14 pixels along the circumference of the lumen on 3 consecutive frames with or without confluent dense calcium.	
FC	>600 µm thick, confluent dense calcium, no confluent necrotic core	

Figure 2. Intravascular ultrasound virtual histology (IVUS-VH) classification system for plaque phenotypes. AIT: adaptative intimal thickening; PIT: pathological intimal thickening; FC: fibrocalcific; FA: fibroatheroma; TCFA: thin-cap fibroatheroma

gorical variables are presented as mean ± standard deviation (SD) and median and interquartile range (IQR) as appropriate. Gray-scale IVUS, plaque composition and lesion phenotype data were compared between the left main, LAD and different LAD segments using the Kruskal-Wallis test (continuous data) and the Chi-square test (categorical data). A *p* value <0.05 was considered significant.

Results

There were 990 patients with complete analysable IVUS images. Among 100 patients who underwent an IVUS evaluation including the proximal LAD and were selected at random for this study, 26 were excluded from the analysis due to short (<30 mm) IVUS pullback in the LAD or lack of complete pullback through the ostium of the left main. Thus, 74 patients (72% male; mean age 65 years) constituted the final population. Baseline characteristics are displayed in **Table 1**. The median LMS length was 5.4 mm (IQR 2.8-8.7 mm).

GEOMETRIC IVUS MEASURES

Compared with the LMS, the proximal LAD had greater PB over the mean length as well as in each 6 mm segment. The plaque volume in the LMS was greater than each LAD segment or the mean plaque volume for the entire LAD pullback length. In contrast, the minimal luminal area (MLA) in the LMS was greater than the median MLA over the proximal 30 mm of the LAD and each individual LAD segment (**Table 2**).

VH-IVUS PLAQUE COMPOSITION

Fibrous tissue was the predominant plaque component of the LMS and LAD with similar percentages in both locations. Fibrofatty plaque composition was larger in the LMS compared to the LAD

Table 1. Population characteristics.

	N=74
Age, y	65.6±10.0
Male	53 (71.6)
Diabetes mellitus	16 (21.6)
Indication for PCI	
Atypical chest pain	8 (11.3)
Stable angina	33 (46.5)
Unstable angina	24 (33.8)
Non-ST-elevation myocardial infarction	3 (4.2)
ST-elevation myocardial infarction	3 (4.2)
Hypertension	51 (68.9)
Dyslipidaemia	50 (67.6)
Previous myocardial infarction	15 (20.3)
Previous coronary artery bypass grafting	2 (2.7)
Congestive heart failure	5 (6.8)
Family history of coronary artery disease	26 (36.1)
Chronic obstructive pulmonary disease	2 (3.3)
Irregular heartbeat	5 (8.2)
Tobacco use	
Current	14 (19.2)
Past	22 (40.0)
Medication use	
Aspirin	58 (79.5)
Clopidogrel	31 (44.3)
Glycoprotein IIb/IIIa	6 (8.1)
Statin	45 (60.8)
Beta blocker	49 (66.2)
Angiotensin converting enzyme inhibitor	30 (40.5)
Calcium channel blocker	12 (16.2)
Other lipid lowering	18 (24.3)
Data are mean ± standard deviation or number (percent)	

Table 2. Geometric, composition, and phenotype measures of atherosclerosis by location.

	Left main (N=74)	Proximal 30 mm					p-value
		6 mm	12 mm	18 mm	24 mm	30 mm	
Grayscale IVUS							
Plaque burden, %	38.5 (33.9-45.2)	49.3 (41.1-53.6)	50.7 (43.0-56.4)	50.5 (44.0-58.2)	49.3 (43.5-58.7)	47.4 (41.0-55.4)	<0.001
Plaque volume, mm ³	27.0 (18.4-42.6)	23.2 (16.5-34.5)	26.3 (17.6-35.4)	23.2 (13.7-36.0)	20.1 (11.9-33.9)	17.5(10.3-26.1)	<0.001
Minimum lumen area, mm ²	12.9 (9.6-15.7)	7.2 (5.8-8.74)	6.7 (4.8-7.9)	5.7 (4.7-7.2)	5.1 (4.0-7.5)	4.8 (4.0-6.7)	<0.001
Plaque composition (%)							
Fibrous	60.3 (52.1-65.1)	60.1 (52.0-65.4)	61.9 (53.6-68.0)	58.8 (51.1-66.1)	58.0 (50.8-66.5)	61.4 (55.2-67.7)	0.10
Fibrofatty	27.9 (20.0-39.2)	16.7 (10.9-24.7)	19.5 (12.3-24.9)	17.6 (11.3-22.3)	14.5 (9.7-22.4)	14.4 (9.8-24.2)	<0.001
Dense calcium	2.5 (0.9-4.7)	6.9 (2.6-12.5)	6.2 (2.3-9.5)	7.2 (4.2-12.4)	7.5 (4.0-16.8)	6.3 (2.6-12.4)	<0.001
Necrotic core	8.0 (3.7-11.8)	13.7 (6.3-18.5)	12.5 (6.5-17.2)	13.3 (9.3-18.6)	14.2 (8.7-19.8)	13.4 (7.5-18.0)	<0.001
Plaque phenotypes (%)*							
Pathological intimal thickening	20.0 (5.3-46.7)	0.0 (0.0-33.3)	8.3 (0.0-33.3)	5.9 (0.0-27.8)	6.3 (0.0-18.8)	8.3 (0.0-28.6)	0.03
Fibroatheroma	16.7 (0.0-40.0)	20.0 (0.0-50.0)	25.0 (8.3-41.7)	21.4 (7.1-37.5)	16.7 (0.0-42.9)	18.2 (0.0-40.0)	0.71
Thin cap fibroatheroma	0.0 (0.0-6.7)	0.0 (0.0-33.3)	14.3 (0.0-43.8)	12.5 (0.0-46.2)	9.1 (0.0-33.3)	9.1 (0.0-33.3)	<0.001

Data are median (interquartile range) *Adaptive intimal thickening and fibrocalcific were undetectable in the left main and proximal 30 mm

segments. The percentages of dense calcium and necrotic core were much lower in the LMS compared to the LAD. The necrotic core content peaked at 14.2% in the fourth 6 mm LAD segment (**Table 2**).

VH-IVUS PLAQUE PHENOTYPE CLASSIFICATION

Adaptive intimal thickening and the more advanced fibrocalcific plaque type were absent in the LMS or proximal 30 mm of the LAD. The distribution of fibroatheroma plaques was similar in the LMS and LAD. Pathological intimal thickening was more common in the LMS than the proximal LAD. TCFA was undetectable in the LMS and first 6 mm LAD segment, its frequency peaked at 14.3% in the second 6 mm and tapered off in the remaining 18 mm LAD segment (**Figure 3**).

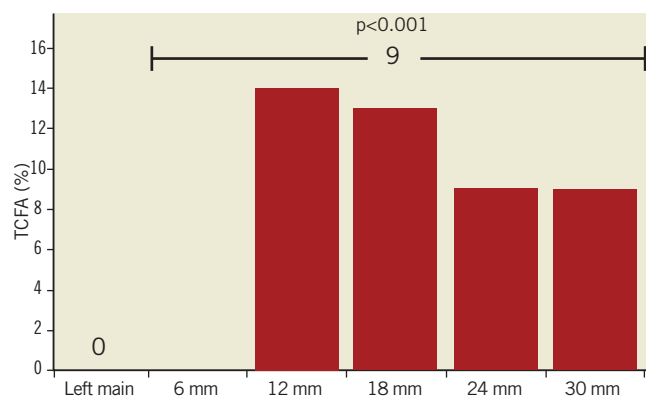


Figure 3. Thin cap fibroatheroma (TCFA) frequency distribution. The frequency of TCFA is presented in the left main stem as well as the proximal 30 mm, divided by 6 mm segments. TCFA was present in 9% of the entire proximal 30 mm.

Discussion

The main findings of the present study are: 1) The LMS has significantly lower PB than the proximal LAD; 2) The volume of necrotic core occurs at much lower frequencies in the LMS compared to the LAD; and 3) TCFA was absent in the LMS and the frequency increased in the proximal LAD and peaked in the second and third 6 mm LAD segments, respectively.

Earlier angiographic studies of the location of plaque rupture causing STEMI suggest that the sites of rupture are clustered in coronary segments within the first 40 mm of the LAD in 90% of the cases³. These findings are consistent with IVUS analyses that showed that LAD plaque ruptures are located 10-40 mm from the LAD ostium in 83% of cases⁴. In pathology studies, plaque rupture distribution appears to be directly related to the distribution of coronary atherosclerosis¹⁶, plaque composition, and TCFA¹⁷, with a greater burden of atherosclerosis and increased frequency of necrotic core and TCFA clustered in more proximal coronary segments but preferentially sparing the LMS.

Our results are consistent with previous analyses where the mean PB of the LMS was approximately 34% but had minimal necrotic core⁵. We extend these findings by identifying that TCFA was absent in the LMS which may explain the lower incidence of LM STEMI in clinical practice or represent a selection bias as complete thrombotic occlusion of the LMS as a result of plaque rupture may be more often fatal, which could explain the high frequency of LMS TCFA in sudden cardiac death patients in autopsy studies¹⁸. On the other hand, ruptured LMS plaques presenting to the cardiac catheterisation laboratory have a sub-occlusive thrombi that rarely compromises the lumen of the LMS¹⁹. Therefore, the presence of TCFA in patients with angiographically mild coronary lesions may serve as a predictor of long term adverse cardiovascular events as recently suggested by the PROSPECT trial²⁰.

The main limitations of this retrospective analysis are its small sample size, lack of post procedural clinical follow-up, which hampers our ability to link VH-IVUS findings with clinical outcomes data; and serial VH-IVUS measurements. However, recent analyses demonstrated a positive correlation between the risk of clinical events derived from three risk-score algorithms for primary prevention and the extent of plaque progression in the LMS measured by serial IVUS, which translates into stenosis progression with increasing clinical risk²¹. It is also important to acknowledge that we excluded the site of the LMS bifurcation segment in this analysis. IVUS analyses have demonstrated that a high percentage of patients with an angiographically normal LMS bifurcation have atherosclerosis at the bifurcation site²². The distribution of atherosclerosis is diffuse rather than focal and both sides of the flow divider (carina) are usually spared²³. Also, percent necrotic core was greatest at the bifurcation compared with the proximal segment of the left main, suggesting a non-uniform distribution at the bifurcation²⁴.

Conclusions

TCFA was present more frequently in the proximal LAD than LMS, supporting the notion that plaque rupture occurs in non-uniform locations throughout the coronary tree and preferentially spares the LMS.

Acknowledgements

We thank Joseph Murphy and Jose Aceituno for publication assistance.

Conflict of interest statement

Dr. Marso reports no personal conflict of interest within the past 12 months. His institution has received consulting fees from The Medicines Company, Novo Nordisk, and Abbott Vascular; research support from The Medicines Company, Amylin Pharmaceuticals, Boston Scientific, Volcano Corporation, and Terumo Medical. Dr. Pieper is a consultant for Volcano Corporation. Dr. Lindsey is a consultant for Novo Nordisk. Dr Stolker is on the speaker's bureau for AstraZeneca. The other authors have no conflicts of interest to declare.

References

- Ambrose JA, Tannenbaum MA, Alexopoulos D, Hjelm Dahl-Monsen CE, Leavy J, Weiss M, Borricco S, Gorlin R, Fuster V. Angiographic progression of coronary artery disease and the development of myocardial infarction. *J Am Coll Cardiol* 1988;12:56-62.
- Libby P, Theroux P. Pathophysiology of coronary artery disease. *Circulation* 2005;111:3481-3488.
- Wang JC, Normand SL, Mauri L, Kuntz RE. Coronary artery spatial distribution of acute myocardial infarction occlusions. *Circulation* 2004;110:278-284.
- Hong MK, Mintz GS, Lee CW, Lee BK, Yang TH, Kim YH, Song JM, Han KH, Kang DH, Cheong SS, Song JK, Kim JJ, Park SW, Park SJ. The site of plaque rupture in native coronary arteries: a three-vessel intravascular ultrasound analysis. *J Am Coll Cardiol* 2005;46:261-265.

- Valgimigli M, Rodriguez-Granillo GA, Garcia-Garcia HM, Vaina S, De Jaegere P, De Feyter P, Serruys PW. Plaque composition in the left main stem mimics the distal but not the proximal tract of the left coronary artery: influence of clinical presentation, length of the left main trunk, lipid profile, and systemic levels of C-reactive protein. *J Am Coll Cardiol* 2007;49:23-31.
- Mintz GS, Nissen SE, Anderson WD, Bailey SR, Erbel R, Fitzgerald PJ, Pinto FJ, Rosenfield K, Siegel RJ, Tuzcu EM, Yock PG. American College of Cardiology Clinical Expert Consensus Document on Standards for Acquisition, Measurement and Reporting of Intravascular Ultrasound Studies (IVUS). A report of the American College of Cardiology Task Force on Clinical Expert Consensus Documents. *J Am Coll Cardiol* 2001;37:1478-1492.
- Whittaker E, Robinson G. The trapezoid and parabolic rules. The calculus of observations: A treatise on numerical mathematics. 4th Edition ed. New York: Dover Publications; 1967:156-158.
- Abramowitz M, Stegun I. Handbook of mathematical functions with formulas, graphs, and mathematical tables. New York: Dover Publications; 1972.
- Fujii K, Carlier SG, Mintz GS, Wijns W, Colombo A, Bose D, Erbel R, de Ribamar Costa J Jr, Kimura M, Sano K, Costa R A, Lui J, Stone GW, Moses JW, Leon MB. Association of plaque characterization by intravascular ultrasound virtual histology and arterial remodeling. *Am J Cardiol* 2005;96:1476-1483.
- Nasu K, Tsuchikane E, Katoh O, Vince DG, Virmani R, Surmely JF, Murata A, Takeda Y, Ito T, Ehara M, Matsubara T, Terashima M, Suzuki T. Accuracy of in vivo coronary plaque morphology assessment: a validation study of in vivo virtual histology compared with in vitro histopathology. *J Am Coll Cardiol* 2006;47:2405-2412.
- Nair A, Kuban BD, Obuchowski N, Vince DG. Assessing spectral algorithms to predict atherosclerotic plaque composition with normalized and raw intravascular ultrasound data. *Ultrasound Med Biol* 2001;27:1319-1331.
- Nair A, Kuban BD, Tuzcu EM, Schoenhagen P, Nissen SE, Vince DG. Coronary plaque classification with intravascular ultrasound radiofrequency data analysis. *Circulation* 2002;106:2200-2206.
- Nair A, Calvetti D, Vince DG. Regularized autoregressive analysis of intravascular ultrasound backscatter: improvement in spatial accuracy of tissue maps. *IEEE Trans Ultrason Ferroelectr Freq Control* 2004;51:420-431.
- Virmani R, Kolodgie FD, Burke AP, Farb A, Schwartz SM. Lessons from sudden coronary death: a comprehensive morphological classification scheme for atherosclerotic lesions. *Arterioscler Thromb Vasc Biol* 2000;20:1262-1275.
- Garcia-Garcia HM, Mintz GS, Lerman A, Vince DG, Margolis M P, van ES GA, Morel MA, Nair A, Virmani R, Burke AP, Stone GW, Serruys P. Tissue characterisation using intravascular radiofrequency data analysis: recommendations for acquisition, analysis, interpretation and reporting. *EuroIntervention* 2009;5:177-189.
- Hochman JS, Phillips WJ, Ruggieri D, Ryan SF. The distribution of atherosclerotic lesions in the coronary arterial tree: relation to cardiac risk factors. *Am Heart J* 1988;116:1217-1222.

17. Cheruvu PK, Finn AV, Gardner C, Caplan J, Goldstein J, Stone GW, Virmani R, Muller JE. Frequency and distribution of thin-cap fibroatheroma and ruptured plaques in human coronary arteries: a pathologic study. *J Am Coll Cardiol* 2007;50:940-949.
18. Kolodgie FD, Burke AP, Farb A, Gold HK, Yuan J, Narula J, Finn AV, Virmani R. The thin-cap fibroatheroma: a type of vulnerable plaque: the major precursor lesion to acute coronary syndromes. *Curr Opin Cardiol* 2001;16:285-292.
19. Tyczynski P, Pregowski J, Mintz GS, Witkowski A, Kim SW, Waksman R, Satler L, Pichard A, Kalinczuk L, Maehara A, Weissman NJ. Intravascular ultrasound assessment of ruptured atherosclerotic plaques in left main coronary arteries. *Am J Cardiol* 2005;96:794-798.
20. Stone GW, Maehara A, Lansky AJ, de Bruyne B, Cristea E, Mintz GS, Mehran R, McPherson J, Farhat N, Marso SP, Parise H, Templin B, White R, Zhang Z, Serruys PW. A Prospective Natural-History Study of Coronary Atherosclerosis. *N Engl J Med* 2011;364: 226-235.
21. von Birgelen C, Hartmann M, Mintz GS, van Houwelingen KG, Deppermann N, Schmermund A, Bose D, Eggebrecht H, Neumann T, Gossel M, Wieneke H, Erbel R. Relationship between cardiovascular risk as predicted by established risk scores versus plaque progression as measured by serial intravascular ultrasound in left main coronary arteries. *Circulation* 2004;110:1579-1585.
22. Hermiller JB, Buller CE, Tenaglia AN, Kisslo KB, Phillips HR, Bashore TM, Stack RS, Davidson CJ. Unrecognized left main coronary artery disease in patients undergoing interventional procedures. *Am J Cardiol* 1993;71:173-176.
23. Oviedo C, Maehara A, Mintz GS, Araki H, Choi SY, Tsujita K, Kubo T, Doi H, Templin B, Lansky AJ, Dangas G, Leon MB, Mehran R, Tahk SJ, Stone GW, Ochiai M, Moses JW. Intravascular ultrasound classification of plaque distribution in left main coronary artery bifurcations: where is the plaque really located? *Circ Cardiovasc Interv* 2010;3:105-112.
24. Han SH, Puma J, Garcia-Garcia HM, Nasu K, Margolis P, Leon MB, Lerman A. Tissue characterisation of atherosclerotic plaque in coronary artery bifurcations: an intravascular ultrasound radiofrequency data analysis in humans. *EuroIntervention* 2010;6: 313-320.